

# Transport of one-dimensional interfaces in the Heisenberg model

Tom Michoel

*Institute for Theoretical Physics, Katholieke Universiteit Leuven,  
Celestijnenlaan 200D, B-3001 Leuven, Belgium*<sup>\*</sup>

Bruno Nachtergael

*Department of Mathematics, University of California,  
Davis, One Shields Avenue, Davis, CA 95616-8366, USA*<sup>†</sup>

Wolfgang Spitzer

*Institut für Theoretische Physik, Universität Erlangen-Nürnberg, 91058 Erlangen, Germany*<sup>‡</sup>

(Dated: May 26, 2019)

We study the transport of one-dimensional interface states in the ferromagnetic Heisenberg model by a time dependent magnetic field. Our analysis is based on the standard adiabatic theorem. This is supplemented by a numerical analysis via the recently developed time dependent DMRG method, where we calculate the adiabatic constant as a function of the strength of the magnetic field and the anisotropy of the interaction.

PACS numbers: 75.10.Pq, 75.40.Gb, 75.60.Ch

## I. INTRODUCTION

The problem of calculating the dynamics of quantum spin chains has acquired new importance due to potential new applications in spintronics [1, 2], quantum information, computation and control theory and the now realistic possibility of doing experiment on systems that are accurately described by a one-dimensional array of spins [8, 18]. The development of time-dependent version of the successful Density Matrix Renormalization Group (DMRG) method of White [20] by several authors [4, 24, 27] therefore comes at a fortuitous moment.

All numerical schemes for a quantum many-body problem such as a spin chain necessarily involve a drastic reduction of the high-dimensional Hilbert space to a suitable subspace of relatively modest dimension. The DMRG method does this by approximating the desired states (typically the ground state and low-lying excitations above it) by finitely correlated states [5], also known as generalized valence bond states or matrix product states. The time-dependent DMRG (tdDMRG) method extends this idea by allowing the subspace used in the approximation scheme to depend on time.

Here we are interested in the dynamics of the Heisenberg XXZ chain with kink boundary conditions [19] and a time-dependent external field. The ground states of this model are the so-called kink states which describe an interface between domains of opposite magnetization.

Their degeneracy grows with the length of the chain [7], and is labelled by the position of the kink, or equivalently, the total magnetization which is a conserved quantity. A transverse external field localized at one site can be used to select a unique ground state [3], i.e., such a perturbation pins the kink at a specific site. In this paper, we want to study the motion of the kink under the influence of a time-dependent magnetic field. Typically we use a field supported at one or two sites and moving at a constant speed. For small velocities, we know by the adiabatic theorem that the time-evolution of a ground state will follow the ground state of the time-dependent Hamiltonian. The standard heuristic to identify the adiabatic regime is the smallness of the ratio of the time-derivative of the Hamiltonian over the spectral gap squared. We will verify the usefulness of this criterion by calculating the time evolution of kink states in the XXZ chain under the influence of a time-dependent magnetic field. Needless to say, the dynamics of kink states, which can be regarded as discrete analogues of solitons, is of great interest in its own right. Moreover, they provide a simple dynamical quantum model of sharp magnetic domain walls.

In order to numerically study the quality of the adiabatic approximation and its domain of validity, it is necessary to express the evolved state in the time-dependent eigenbasis of the Hamiltonian. Therefore we construct the DMRG basis at time  $t$  starting from the ground state(s) and low-lying excited states of the Hamiltonian of the system at time  $t$ . This is in contrast with the original method, where the time-dependent DMRG basis is obtained from the evolved state at time  $t$ . Our method can be of more general interest, since the calculation of the DMRG basis is a separate calculation about which we can be confident to have good control, regardless of the potential difficulties in reliably calculating the time evolution.

The paper is organized as follows. In Section II, we

---

<sup>\*</sup>Current address: Bioinformatics & Evolutionary Genomics, Department of Plant Systems Biology, VIB/Ghent University, B-9052 Gent, Belgium; Electronic address: tom.michoel@psb.ugent.be

<sup>†</sup>Electronic address: bxn@math.ucdavis.edu

<sup>‡</sup>Electronic address: Wolfgang.Spitzer@physik.uni-erlangen.de;

© 2006 by the authors. This article may be reproduced in its entirety for non-commercial purposes.

define the model and study its basic properties. The adiabatic approximation is studied in Section III. In Section IV, we give a brief discussion of the issues that arise with rapidly changing magnetic fields. Details of the DMRG algorithm, including error analysis, are given in Section V.

## II. THE MODEL

The spin- $\frac{1}{2}$  ferromagnetic XXZ Heisenberg model<sup>1</sup> on the chain  $[1, L]$  with interface boundary conditions is defined by the Hamiltonian  $H_0 = \sum_{x=1}^{L-1} h_{x,x+1}$ , with nearest-neighbor interaction

$$h_{x,x+1} = -\frac{1}{\Delta}(S_x^1 S_{x+1}^1 + S_x^2 S_{x+1}^2) - S_x^3 S_{x+1}^3 + \frac{1}{2}\sqrt{1-\Delta^{-2}}(S_x^3 - S_{x+1}^3) + \frac{1}{4}\mathbb{1},$$

where  $\Delta > 1$  is the anisotropy parameter and the matrices  $\mathbf{S}_x = (S_x^1, S_x^2, S_x^3)$  are the usual spin- $\frac{1}{2}$  matrices,

$$S_x^1 = \frac{1}{2} \begin{pmatrix} 0 & 1 \\ 1 & 0 \end{pmatrix}, \quad S_x^2 = \frac{1}{2} \begin{pmatrix} 0 & 1 \\ -1 & 0 \end{pmatrix}, \quad S_x^3 = \frac{1}{2} \begin{pmatrix} 1 & 0 \\ 0 & -1 \end{pmatrix}.$$

We have added the term  $\frac{1}{4}\mathbb{1}$  so that  $h_{x,x+1}$  is positive (in fact, it is a projection) and  $H_0$  has ground state energy 0.

The Hamiltonian  $H_0$  acts on the Hilbert space  $\mathcal{H}_L = \mathbb{C}^{2^L}$ . It has a large (quantum) symmetry with a similar multiplet structure as the  $SU(2)$ -symmetric, isotropic model where  $\Delta = 1$ . In the limit  $\Delta \rightarrow \infty$  we obtain the Ising Model,  $H^{\text{Ising}} = H_0(\Delta = \infty)$ . The ground states and excited states (for finite  $L$  and in the infinite volume limit  $L \rightarrow \infty$ ) have been analyzed completely in recent years [12, 13, 15, 16, 17]. A convenient basis of ground states are the so-called grand canonical ground states,  $\phi(z)$ . They are product states and depend on a complex parameter  $z \in \mathbb{C} \setminus \{0\}$ :

$$\phi(z) = \bigotimes_{x=1}^L \left[ (1 + |z|^2 q^{2x})^{-1/2} \begin{pmatrix} 1 \\ zq^x \end{pmatrix} \right]. \quad (1)$$

The state  $\phi(z)$  describes an interface state that is exponentially localized at  $x_0 = -\ln|z|/\ln q$  with  $q = \Delta - \sqrt{\Delta^2 - 1} \in (0, 1)$ . The width depends on  $\Delta$  as shown by the following estimates for the magnetization profile:

$$\begin{aligned} \frac{1}{2} - \langle \phi(z) | S_x^3 | \phi(z) \rangle &\leq q^{2|x-x_0|} \quad \text{for } x > x_0, \\ \frac{1}{2} + \langle \phi(z) | S_x^3 | \phi(z) \rangle &\leq q^{2|x-x_0|} \quad \text{for } x < x_0. \end{aligned}$$

The interface becomes sharp (i.e., the transition from up to down spin occurs across one bond) in the Ising limit

$\Delta \rightarrow \infty$  and becomes flat as  $\Delta \downarrow 1$ , and there are no interface states in the isotropic Heisenberg model.

We perturb the Hamiltonian by a magnetic field defined by a function  $\mathbf{B} : [1, L] \rightarrow \mathbb{R}^3$  satisfying

(A1) The support of  $\mathbf{B}$  is finite independent of  $L$ .

(A2) The field is of the form,

$$\mathbf{B}(x) = (B^1(x), 0, B^3(x)),$$

where  $B^1$  is a non-zero, non-positive function.

Note that by applying a global rotation around the  $z$ -axis, fields of a slightly more general form can be considered as well.

Then we define

$$H_V = H_0 + V \quad \text{with} \quad V = \sum_x \mathbf{B}(x) \cdot \mathbf{S}_x. \quad (2)$$

We refrain from considering the infinite chain limit in detail. The first condition on the support of  $V$  is to ensure that  $H_V$  is still a well-defined semi-bounded operator in the GNS representation of the *unperturbed* Hamiltonian. The second assumption makes sure that the ground state of  $H_V$  will be an interface state, in the sense that to the left/right of the support of  $V$ , the profile is asymptotically equal to  $-\frac{1}{2}$ , respectively  $\frac{1}{2}$ . If  $\mathbf{B}(x) = (0, 0, B_x)$  with  $B_x \geq 0$ , the ground state is the all spin-up state which is then part of the continuous spectrum of  $H_V$ , see the discussion in [3].

The case of a magnetic field located at a *single* site  $y$  has been analyzed in [3]. Let

$$\phi_y = \phi \left( -\frac{\|\mathbf{B}\| + B_3}{B_1 - iB_2} q^y \right)$$

be a state of the form (1). If  $\mathbf{B} = (B, 0, 0)$  with  $B < 0$ , then  $\phi_y$  is a kink localized at site  $y$ . The state  $\phi_y$  has energy  $-\frac{1}{2}\|\mathbf{B}\|$ , and since the ground state energy can be at most shifted by this amount, we know that it is a ground state. It is also the unique ground state which moreover has a uniform gap as  $L \rightarrow \infty$ . In the present situation we generalize this to extended magnetic fields.

**THEOREM II.1.** *Let  $\mathbf{B}$  satisfy the above conditions (A1) and (A2). Then,*

1.  *$H_V$  from (2) has a unique ground state,  $\phi$ , with ground state energy  $E_0$ .*
2. *There exists a finite  $\Delta_0 = \Delta_0(\mathbf{B})$  so that for  $\Delta > \Delta_0$ , there is a positive and in  $L$  uniformly bounded gap above the ground state. I.e., there exists a  $\gamma > 0$  independent of  $L$  so that for all states  $\psi$  orthogonal to the ground state  $\phi$  we have  $\langle \psi | (H_V - E_0) | \psi \rangle \geq \gamma \|\psi\|^2$ .*

We believe that a positive gap persists for all  $\Delta > 1$ . Here we only show the result for sufficiently large  $\Delta$  by a simple perturbative argument.

<sup>1</sup> We set  $\hbar = 1$  which should be kept in mind when we define adiabatic regimes in terms of the magnitude of the magnetic field and the velocity.

*Proof.* Let  $\mathbf{B}(x) = (B^1(x), 0, B^3(x))$ . Since  $B^1 \leq 0$ , the operator  $H_V = H_0 + V$  has non-positive off-diagonals in the Ising basis, and acts irreducibly in this basis. Hence, by the Perron-Frobenius theorem,  $H_V$  has a unique ground state,  $\phi$ .

For the second part, let us define  $H_V^{\text{Ising}} = H_V(\Delta = \infty)$ , the Ising kink Hamiltonian with the magnetic field  $\mathbf{B}$ . If the support of  $\mathbf{B}$  is contained in the interval  $[\ell, r]$ , then the ground state  $\psi_0$  of  $H_V^{\text{Ising}}$  on the chain  $[1, L]$  is equal to the ground state of  $H_V^{\text{Ising}}$  on the subchain  $[\ell-1, r+1]$  times the all spin-down state to the left of  $\ell-1$  and all spin-up state to the right of  $r+1$ . The ground state energy  $E_0$  and the gap of  $H_V^{\text{Ising}}$  are independent of  $L$ .

To first order in  $q$ , the XXZ Hamiltonian  $H_V = H_V(q)$  equals  $H_V^{\text{Ising}} + qH_1$  with

$$H_1 = - \sum_{x=1}^{L-1} (S_x^1 S_{x+1}^1 + S_x^2 S_{x+1}^2).$$

Let  $\psi(q)$  be the ground state of  $H_V(q)$  with energy  $E_0(q)$ . Then to first order  $\psi(q) = \psi_0 + q\psi_1$  and  $E_0(q) = E_0 + qE_1$ . If we insert this into the eigenvalue equation,  $(H_V(q) - E_0(q))\psi(q) = 0$  we get that  $E_1 = \langle \psi_0 | H_1 | \psi_0 \rangle$  which is independent of  $L$ . Thus for small  $q$ , or equivalently large  $\Delta$ , there is a uniform gap above the ground state.  $\square$

Our prime example will be magnetic fields located on two adjacent sites,  $x_0 = L/2$  and  $x_0 + 1$ . More precisely, let  $v, B > 0$  and define

$$B(x, t) = -B \cdot f(x - vt)$$

$$f(x) = \begin{cases} 1 - |x - x_0| & \text{for } x_0 - 1 \leq x \leq x_0 + 1 \\ 0 & \text{else} \end{cases}$$

The perturbation

$$V(t) = \sum_{x=1}^L B(x, t) S_x^1 = (1 - vt) B S_{x_0}^1 + vt B S_{x_0+1}^1 \quad (3)$$

for  $0 \leq t \leq \tau = 1/v$  obviously satisfies the conditions **(A1)** and **(A2)**. Hence, we know from Theorem II.1 that the Hamiltonian,

$$H(t) = H_0 + V(t) \quad (4)$$

has a unique ground state,  $\phi(t)$ , with a positive gap. The ground state energy  $E_0(t, B)$  is analytic on  $(0, v^{-1})$ , also as  $L \rightarrow \infty$ ; this is a special case of the more general fact that isolated eigenvalues of finite degeneracy are analytic upon relatively bounded perturbations, see [22, 3.5.14].

It is another well-known fact [22, 3.5.23] that the ground state energy  $E_0(t, B)$  is concave in  $t$ . By symmetry we also have  $E_0(t, B) = E_0(v^{-1} - t, B)$  for  $0 \leq t \leq 1/(2v)$ . This implies  $E_0(1/2v, B) = \max_t E_0(t, B)$ . We can get more information on  $E_0(t, B)$  from the low energy spectrum of the Hamiltonian with the magnetic field at a *single* site. For simplicity we put  $v = 1$ .

**PROPOSITION II.2.** *Let  $g(t)^2$  be the gap above the ground state  $\phi_y$  of  $H_y(t) = H_0 - tBS_y^1$ . Then<sup>3</sup>  $g(t)$  is increasing in  $t$ . Further, on  $[0, 1/2]$  we have*

$$H(t) \geq \frac{1}{2}g(2t) (1 - |\langle \phi_x | \phi_{x+1} \rangle|).$$

*Proof.* That  $g(t)$  is increasing follows from the variational principle. To this end, let  $0 < t < t'$ . Let  $\psi$  be orthonormal to  $\phi_y$  such that  $\langle \psi | H_y(t') - t' B / 2 | \psi \rangle = g(t')$ . Then,

$$\begin{aligned} \langle \psi | H_y(t) - t' B / 2 | \psi \rangle \\ = g(t') - (t - t') B \langle \psi | S_y^1 + \frac{1}{2} \mathbb{1} | \psi \rangle \leq g(t'). \end{aligned}$$

Thus,  $g(t) \leq g(t')$ .

The estimate on the ground state energy of  $H(t)$  is based on Kitaev's Lemma (see [11, Lemma 14.4]). In general, let  $A_1$  and  $A_2$  be two operators on some Hilbert space  $\mathcal{H}$ . By  $G_{1,2}$  and  $\Pi_{1,2}$  we denote the space of ground states and the orthogonal projections onto  $G_{1,2}$ , respectively. We assume that  $G_1 \cap G_2 = \{0\}$ , and that for some  $\delta > 0$ ,  $A_{1,2} \geq \delta(1 - \Pi_{1,2})$ . Then,

$$A_1 + A_2 \geq \delta \left( 1 - \sup_{\psi_{1,2} \in G_{1,2}} |\langle \psi_1 | \psi_2 \rangle| \right).$$

For our proof it suffices to apply this inequality with

$$\begin{aligned} A_1 &= \frac{1}{2}H_0 - (1 - t)B(S_x^1 + \frac{1}{2}\mathbb{1}) \\ &= \frac{1}{2}H_x(2(1 - t)) - \frac{1}{2}(1 - t)B\mathbb{1}, \\ A_2 &= \frac{1}{2}H_0 - tB(S_{x+1}^1 + \frac{1}{2}\mathbb{1}) = \frac{1}{2}H_x(2t) - \frac{1}{2}tB\mathbb{1}. \end{aligned}$$

$\square$

We supplement this analysis of the ground state properties of the family of Hamiltonians (4) with numerical DMRG calculations for a chain of length  $L = 20$  and an anisotropy of  $\Delta = 2$ . The chain length should be chosen such that for given  $\Delta$ ,  $L$  is much larger than the width of the interface, but otherwise there are no qualitative differences for different combinations of  $\Delta$  and  $L$ . In order to deal with non-translation invariant kink states, a few modifications are needed with respect to the standard ground state DMRG algorithm [26]. Those are outlined in Section V.

We distinguish three ranges of  $B$ -values with qualitatively different ground state properties.

*a. Intermediate  $B$*  A typical intermediate value of  $B$  is 0.5. In Figure 1, we see that the  $S^3$ -magnetization profile of the ground states  $\varphi(t)$  of  $H(t)$  nicely interpolates between the interface product states  $\varphi(0)$  and  $\varphi(1)$  of type defined in eq. (1), localized at  $x_0 = 10$ , resp.  $x_0 + 1 = 11$ , and that the first excited states are still well localized around the interface positions.

<sup>2</sup> We set  $g(0) = 0$ .

<sup>3</sup> Strictly speaking,  $g(t)$  also depends on  $L$  which we will tacitly ignore.

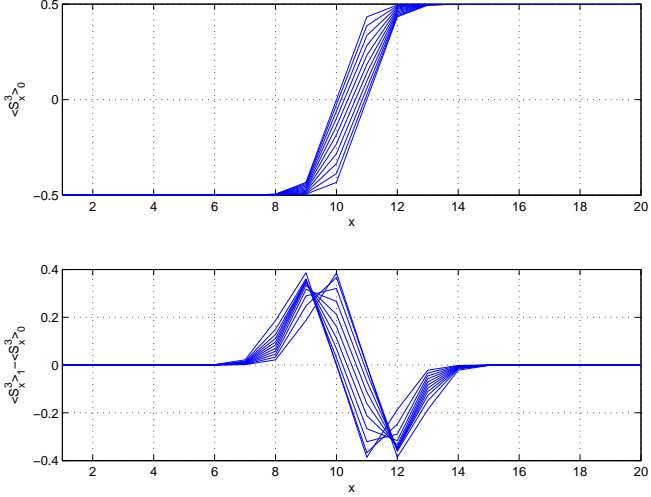


FIG. 1:  $S^3$ -magnetization profiles of the ground states (top) and difference of  $S^3$ -magnetization profiles of the first excited and ground states (bottom), for  $0 \leq t \leq \tau$  ( $B = 0.5$ ,  $\tau = 200$ , 200 time steps, profiles plotted for every 20 time steps).

The transition from  $\varphi(0)$  to  $\varphi(1)$  is however not homogeneous, in the sense that the right or top half of the interface moves first and the left or lower half moves later, see Figure 2. This effect becomes more pronounced as  $B$  increases (compare Figure 2 and Figure 5) and can be understood as follows. In the first phase after switching on a magnetic field at  $x_0 + 1$ ,  $S_{x_0+1}^1$  has the effect of rotating the up vector at  $x_0 + 1$  into the  $(1, 2)$ -plane. But here nothing happens at site  $x_0$  because the initial state is an eigenstate of  $S_{x_0}^1$ . The same thing happens at the end of the cycle when the vector at  $x_0 + 1$  is almost an eigenvector of  $S_{x_0+1}^1$ . Site  $x_0$  is effected only after some time as the perturbation at  $x_0 + 1$  is communicated to  $x_0$  in second order.

In Figure 3, we see that both the ground and first excited state energies are concave as a function of  $t$ , and that the ground state energy is minimal and equal to the known value  $-B/2$  at the start ( $t = 0$ ) and end ( $t = \tau$ ) points. The gap is always strictly positive, but minimal at half period ( $t = \tau/2$ ).

*b. Small  $B$*  For very small magnetic fields, the magnetization profile of the ground and first excited states is very similar to the profiles in Figure 1. The ground state energy is still a concave function of  $t$ , but the first excited state energy is now convex, see Figure 4. The energy gap however is still minimal at half period. Furthermore the energy gap for a 10 times smaller magnetic field (0.05 vs. 0.5) is approximately 10 times smaller, confirming the theoretical result [3] (for a single site impurity) that the gap scales linearly with  $B$  for small  $B$ .

*c. Large  $B$*  For magnetic fields much larger than the intermediate value  $B \sim 0.5$ , the phenomenon that the interface moves in separate steps, first the right half then the left half, becomes much more pronounced, see Figure 5. Like for intermediate  $B$ -values, the energies of the

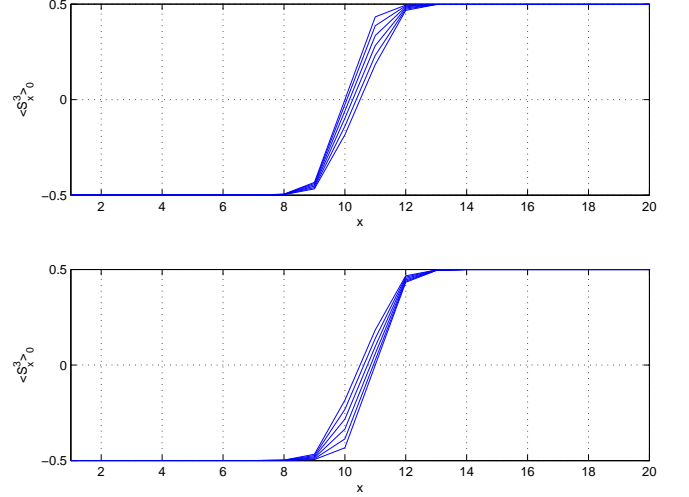


FIG. 2:  $S^3$ -magnetization profile of the ground states, for  $0 \leq t \leq \tau/2$  (top) and  $\tau/2 \leq t \leq \tau$  (bottom) ( $B = 0.5$ ,  $\tau = 200$ , 200 time steps, profiles plotted for every 20 time steps).

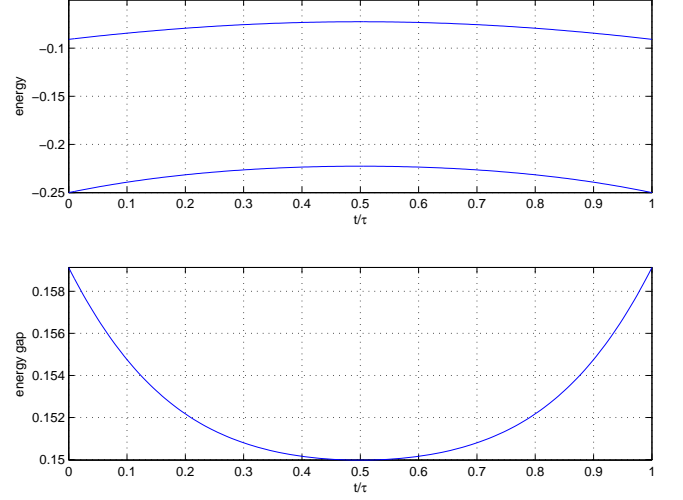


FIG. 3: Energy of the ground states and first excited states (top) and energy gap (bottom) ( $B = 0.5$ ,  $\tau = 200$ , 200 time steps).

ground and first excited states are concave functions of  $t$ , but the minimal gap now occurs at the start and final times (Figure 6).

### III. ADIABATIC TRANSPORT

Let us recall the standard adiabatic theorem which applies also to the case of an infinite chain. Let  $\tau > 0$  and  $H(t)$ ,  $0 \leq t \leq \tau$ , be a family of self-adjoint operators with common dense domain, and let  $\psi(t)$  be the solution to

$$i\frac{\partial}{\partial t}\psi(t) = \tau H(t)\psi(t) \quad (5)$$

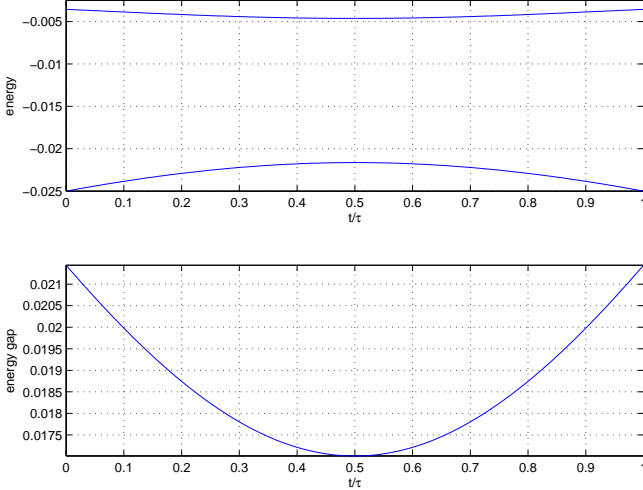


FIG. 4: Energy of the ground states and first excited states (top) and energy gap (bottom) ( $B = 0.05$ ,  $\tau = 200$ , 200 time steps)

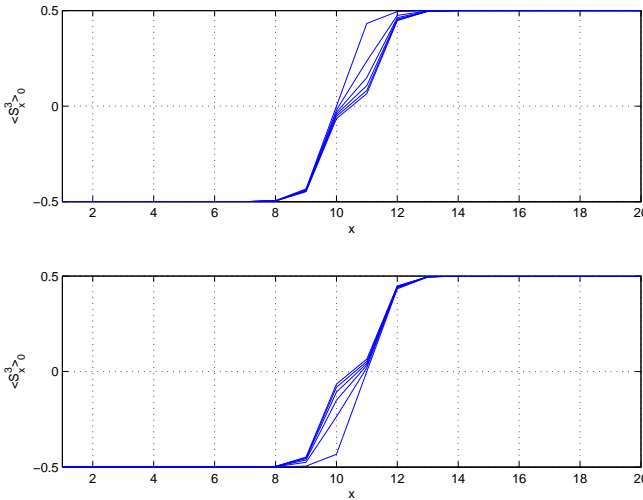


FIG. 5:  $S^3$ -magnetization profile of the ground states, for  $0 \leq t \leq \tau/2$  (top) and  $\tau/2 \leq t \leq \tau$  (bottom) ( $B = 5.0$ ,  $\tau = 200$ , 200 time steps, profiles plotted for every 20 time steps).

with initial condition  $\psi(0)$ . By  $P(t)$  we denote the spectral projection onto the ground states of  $H(t)$ . We assume that  $P(t)$  is piece-wise, twice continuously differentiable, finite dimensional, and uniformly (in  $t$ ) separated from the rest of the spectrum of  $H(t)$  by a gap  $\gamma(t)$ .

**THEOREM III.1** (Adiabatic Theorem, Kato). *Under the above conditions on  $H(t)$  and  $\psi(t)$ , there is an eigenvector  $\varphi(t)$  of  $H(t)$  with  $\varphi(0) = \psi(0)$  and a constant  $C$  such that,*

$$\sup_{0 \leq t \leq \tau^{-1}} \|\psi(t) - \varphi(t)\| \leq C\tau^{-1}. \quad (6)$$

*Proof.* See [10] or [22, 3.3.11]. □

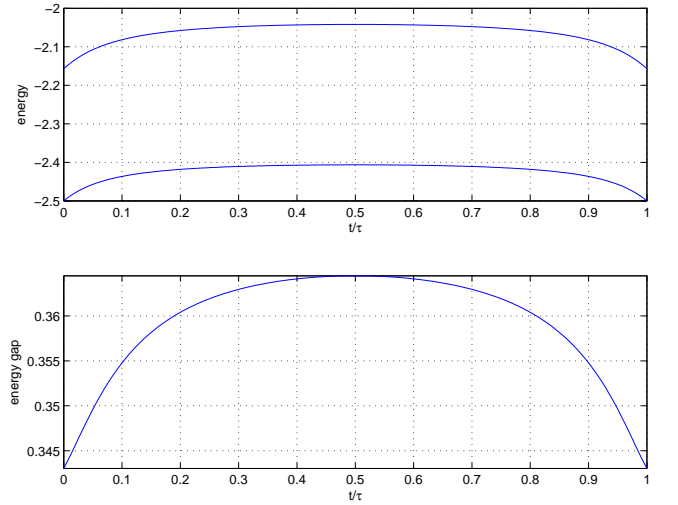


FIG. 6: Energy of the ground states and first excited states (top) and energy gap (bottom) ( $B = 5.0$ ,  $\tau = 200$ , 200 time steps)

We call the smallest constant  $C$  in (6) the adiabatic constant. Heuristically (see [14, 17.112]), the adiabatic constant is of the order

$$\sup_{s \in [0, 1]} \frac{\|\frac{d}{ds} H(s)\|}{\gamma(s)^2}, \quad s = t/\tau. \quad (7)$$

In our case,  $H(t)$  is given by (4), and

$$\|\frac{d}{ds} H(s)\| = \|BS_{x_0}^1 - BS_{x_0+1}^1\| = B.$$

Hence,  $C \propto B/\gamma_{\min}^2$  with  $\gamma_{\min} = \min_{s \in [0, 1]} \gamma(s)$  the minimal gap. Let us take this estimate and look at small and large magnetic fields. As  $B$  tends to infinity the gap  $\gamma$  saturates and therefore  $C$  grows linearly with  $B$  for large  $B$ . On the other hand, if  $B$  is small then the gap shrinks like  $B$  (not  $B^2$ ) as has been shown for a single site perturbation [3]. In other words, if we have fixed  $B$  and  $\Delta$  and some  $\varepsilon$  we can find (empirically) the velocity  $v$  for which then the adiabatic evolution is  $\varepsilon$ -close (in the  $\ell^2$ -sense) to the true time evolution.

On a rigorous level, estimates in the vein of (7) on the adiabatic constant were recently derived by Jansen, Ruskai, and Seiler [9]. For small  $B$  we use the bound in their Theorem 3 which states that

$$C \leq \frac{2B}{\gamma(0)^2} + 7B^2 \int_0^1 \gamma(s)^{-3} ds.$$

By the same argument as above, the right hand side is of the order of  $1/B$  for small  $B$ . For large  $B$ , we rely on the bound in their Theorem 4 which says

$$C \leq \frac{2B}{\gamma(0)^2} + \frac{C'}{\tau} B^4.$$

The constant  $C'$  depends on  $\gamma(s)$  but the dependency is flat for large  $B$ . The second term seems big but is

multiplied with  $1/\tau$ . This can be made arbitrarily small for fixed  $B$  if we choose  $\tau$  large enough.

We have computed the adiabatic constant numerically using adaptive time-dependent DMRG [24, 27]. Since we need to compare the time-evolved state  $\psi(t)$  with the ground state  $\varphi(t)$ , we have developed an alternative version of tdDMRG which adaptively targets the low-energy spectrum of  $H(t)$  and expresses  $\psi(t)$  in this basis along the way. Our algorithm is outlined in Section V.

In Figure 7 and 8, we have plotted the adiabatic constant as well as the heuristic upper bound

$$C \leq \alpha \frac{B}{\min_{s \in [0,1]} \gamma(s)^2},$$

with the energy gaps computed by ground state DMRG (see Section II). To determine  $\alpha$ , we took one value of  $B$  ( $B = 1.0$  for  $\Delta = 2$  and  $B = 2.0$  for  $\Delta = 10$ ) and made the inequality in (7) an equality at the lowest  $v$  ( $v = 0.001$ ) at this particular value of  $B$ .

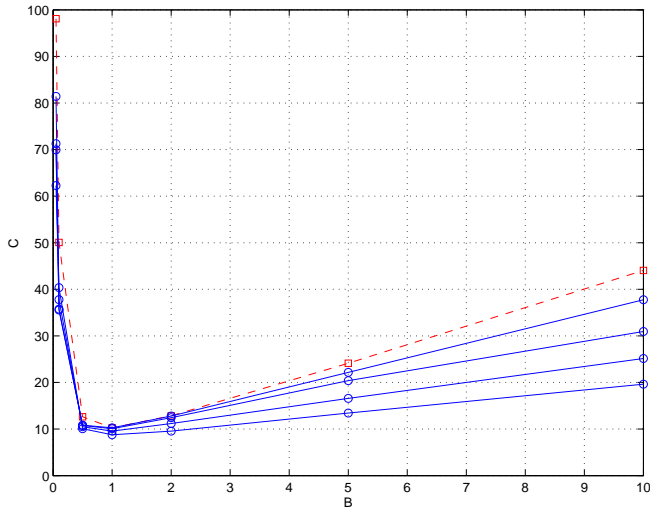


FIG. 7: Adiabatic constant as a function of magnetic field strength  $B$  for different velocities  $v = 0.01, 0.005, 0.002, 0.001$  (solid lines, bottom to top) compared to the upper bound  $\alpha B/\gamma_{\min}^2$  (dashed line) for anisotropy  $\Delta = 2$  ( $\alpha = 0.5677$ ) and  $L = 20$ .

Since our time-dependent algorithm does not target the state  $\psi(t)$  directly, but rather the lowest energy states of the Hamiltonians  $H(t)$  (see Section V), it is important to keep track of how well  $\psi(t)$  is represented in these time-evolving DMRG bases. One way to measure this is by computing the deviation from 1 of the norm of  $\psi(t)$ . As expected there is a correlation between this norm loss and the value of the adiabatic constant  $C$ . In Figure 7 and 8, where  $C$  is minimal,  $\|\psi(t)\|$  will be above 0.999 at all times; at the very smallest and very largest  $B$ -fields, and for the largest velocities still considered adiabatic ( $v \approx 0.01$ ) the minimum norm drops to about 0.97.

Adiabaticity is also measured by comparing the value of the total energy in the time-evolved state with the

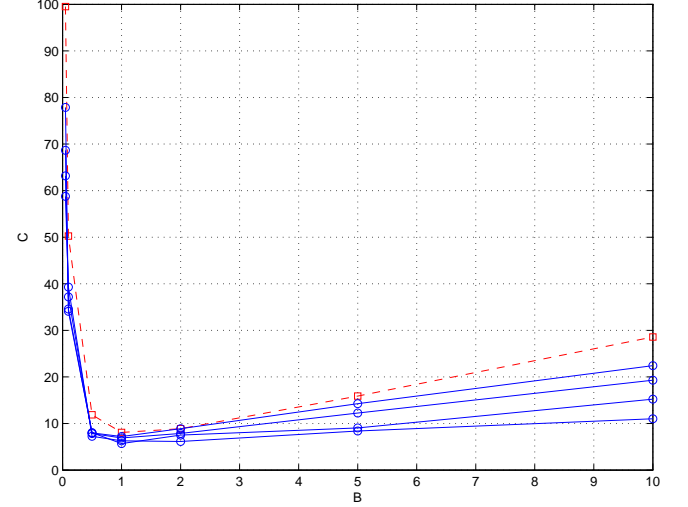


FIG. 8: Adiabatic constant as a function of magnetic field strength  $B$  for different velocities  $v = 0.01, 0.005, 0.002, 0.001$  (solid lines, bottom to top) compared to the upper bound  $\alpha B/\gamma_{\min}^2$  (dashed line) for anisotropy  $\Delta = 10$  ( $\alpha = 0.6324$ ) and  $L = 20$ .

ground state energy of  $H(t)$ , i.e.,

$$\frac{\langle \psi(t) | H(t) | \psi(t) \rangle}{\| \psi(t) \|^2} - E_0(t)$$

should be close to 0 at all times. For a typical adiabatic speed  $v = 0.005$  and intermediate  $B$ -field, this difference never exceeds  $5 \cdot 10^{-4}$ . Energy differences in the small and large  $B$  regions are of similar magnitude.

For large values of the anisotropy  $\Delta$  the interface is so well localized that we can actually reduce the chain length  $L$  to a value where the dynamics can be computed by exact matrix exponentiation and no DMRG is necessary. Figure 9 shows the same comparison between the true adiabatic constants and the upper bound (7). Obviously for smaller  $L$  the convergence to the adiabatic limit is more rapid.

Finally, we want to comment on the role of the interpolation function in our adiabatic Hamiltonian. Let us consider a large magnetic field. Then we see that as time proceeds part of the profile is lagging behind. Also, the change of the profile is rather quick in the beginning (and at the end) and slow in the middle of a cycle. If we want to improve on the transport of the domain wall for a fixed time interval we can take advantage of this phenomenon and slow down the time evolution in the beginning and accelerate in the middle by choosing a different interpolation function than the standard linear scale from (3). In other words, we may use a general interpolating Hamiltonian  $H_f(t) = H_0 - (1 - f(vt))BS_{x_0}^1 - f(vt)BS_{x_0+1}^1$  with the constraint that  $f(1) = 1 - f(0) = 1$  to keep the same mean velocity. As an example we have used the function  $f_1(t) = \cos(\pi t/2)$  and a piece-wise linear function  $f_2$  with slope 1/3 for  $t \in [0, 1/6] \cup [5/6, 1]$  and slope 4/3 on the interval  $[1/6, 5/6]$ . In the first

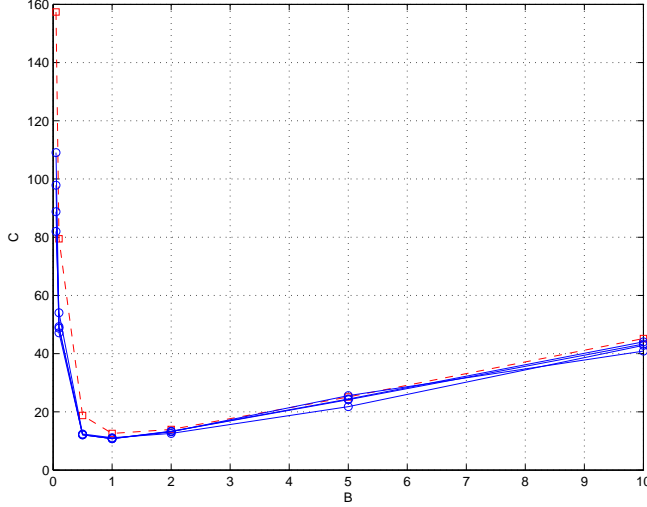


FIG. 9: Adiabatic constant as a function of magnetic field strength  $B$  for different velocities  $v = 0.01, 0.005, 0.002, 0.001$  (solid lines) compared to the theoretical estimate  $\alpha B / \gamma_{\min}^2$  (dashed line) for  $\Delta = 10$  and  $L = 8$  ( $\alpha = 1.0$ ).

case we took  $L = 20, \Delta = 2, B = 5, v = 0.05$  and reduced the adiabatic constant from 16.6 (constant velocity, or equivalently linear  $f$ ) to 4.5 calculated with  $f_1$ . In the second example with  $f_2$  and parameter values  $L = 20, \Delta = 2, B = 10, v = 0.05$  the adiabatic constant dropped from 25.1 to 12.2. This observation is in agreement with [9], where the adiabatic constant for the general interpolating Hamiltonian  $H_f(t)$  was studied.

#### IV. FAST CHANGE OF THE MAGNETIC FIELD

Now we study the situation when the velocity of the moving magnetic field is large. This is based on standard formal results (cf. [14]) since we are not aware of rigorous studies in this regime. We use the same setup as in the previous section. So let  $\phi = \phi_{x_0}$  be the ground state of  $H(0) = H_0 - BS_{x_0}^1$ . Let  $\tau = 1/v$  and let  $p(\tau)$  be the probability that at time  $\tau$  the system is still in the state  $\phi$ . Then according to formula [14, (17.60)],

$$p(\tau) = 1 - \tau^2 \text{var}_\phi(\bar{H}) + \mathcal{O}(\tau^3)$$

with  $\text{var}_\phi(\bar{H}) = \langle \phi | \bar{H}^2 | \phi \rangle - \langle \phi | \bar{H} | \phi \rangle^2$ , and  $\bar{H} = \frac{1}{\tau} \int_0^\tau H(t) dt$ . In our example,  $\bar{H} = H_0 - \frac{B}{2}(S_{x_0}^1 + S_{x_0+1}^1)$ . Since  $\phi$  is also an eigenstate of  $H_0 - \frac{B}{2}S_{x_0}^1$  with energy  $-\frac{B}{4}$ , we obtain

$$\begin{aligned} \langle \phi | \bar{H} | \phi \rangle &= -\frac{B}{4} - \frac{B}{2} \langle \phi | S_{x_0+1}^1 | \phi \rangle, \\ \langle \phi | \bar{H}^2 | \phi \rangle &= \frac{B^2}{8} - \frac{B^2}{2} \langle \phi | S_{x_0+1}^1 | \phi \rangle. \end{aligned}$$

Hence,

$$\text{var}_\phi(\bar{H}) = \frac{B^2}{16} (1 - 4 \langle \phi | S_{x_0+1}^1 | \phi \rangle - 4 \langle \phi | S_{x_0+1}^1 | \phi \rangle^2).$$

The quantity  $\langle \phi | S_{x_0+1}^1 | \phi \rangle$  can be computed fairly explicitly as a function of  $\Delta$  but we are content with the trivial estimate that

$$1 \leq 1 - 4 \langle \phi | S_{x_0+1}^1 | \phi \rangle - 4 \langle \phi | S_{x_0+1}^1 | \phi \rangle^2 \leq 2$$

since  $-\frac{1}{2} \leq \langle \phi | S_{x_0+1}^1 | \phi \rangle \leq 0$  for all  $\Delta \geq 1$ . As a result, the probability to stay in the initial state  $\phi$  until  $\tau$ ,

$$p(\tau) \geq 1 - \frac{\tau^2 B^2}{8} + \mathcal{O}(\tau^3).$$

If we want this to be larger than  $1 - \varepsilon$ , then  $|B|$  needs to be smaller than  $\sqrt{8\varepsilon}v$ .

Numerically we can also investigate the intermediate region between adiabatic and sudden change of the magnetic field. Here,  $B$  and  $v$  are of the same order of magnitude. In Figure 10, we follow the  $S^3$ -magnetization profile of the time evolved state over two periods, with the natural extension of  $V(t)$  in (3) such that the field keeps moving to the right. We see that although the position of the interface is transported in the same direction as the magnetic field, it is lagging behind w.r.t. the position of the ground state interfaces  $\varphi(t)$  (which moves from site 10 to site 12). At the same time the width of the interface is growing bigger.

In this computation, the minimum norm of  $\psi(t)$  remains above 0.99 for the first period ( $t \leq v^{-1}$ ) and above 0.97 for the second period ( $t \leq 2v^{-1}$ ), so despite the non-adiabatic transport,  $\psi(t)$  is still well represented in the DMRG basis constructed from the low-energy spectrum of  $H(t)$ . The overlap with the ground state  $\varphi(t)$  drops to 0.80 during the first period, and further to 0.71 during the second period

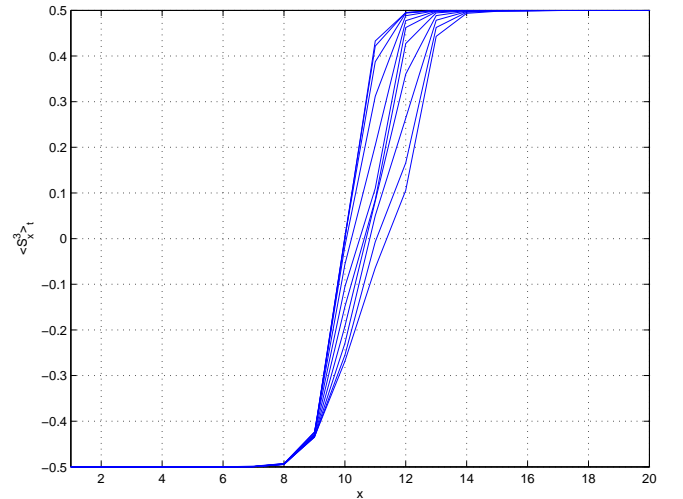


FIG. 10:  $S^3$ -magnetization profiles of  $\psi(t)$ , for  $0 \leq t \leq \tau = 2v^{-1}$  ( $\Delta = 2, B = 0.5, v = 0.1$ , 200 time steps, profiles plotted for every 20 time steps).

In Figure 11, we see how the energy of  $\psi(t)$  evolves over time. Again  $\psi(t)$  is lagging behind w.r.t. the periodicity of the spectrum of  $H(t)$ . The difference with the ground

state energy is steadily increasing (Figure 11, bottom), and it is an interesting question whether this difference will eventually saturate.

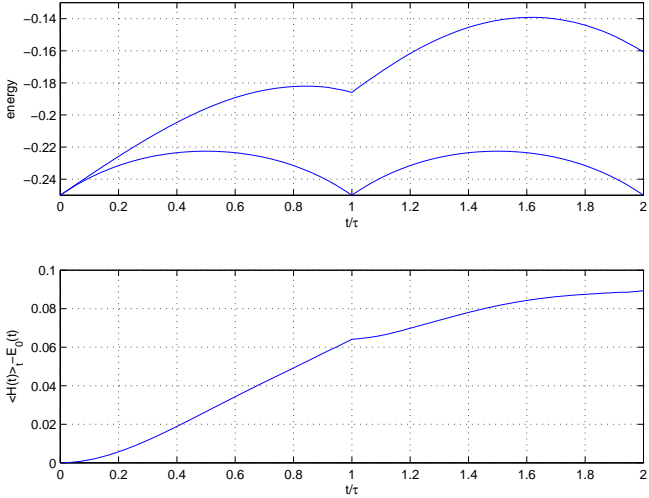


FIG. 11: Ground state energy and energy of  $\psi(t)$  (top) and energy difference between  $\psi(t)$  and the ground state (bottom) ( $\Delta = 2$ ,  $B = 0.5$ ,  $v = 0.1$ , 200 time steps).

We have tested other magnetic field perturbations such as a smooth field

$$V(t) = \frac{B}{4} \sum_x (1 + \cos(\pi(x - vt)))^2 \chi_L(x - vt) S_x^1$$

where

$$\chi_L(x) = \begin{cases} 1 & \text{for } x \in [L/2 - 1, L/2 + 1] \\ 0 & \text{otherwise} \end{cases}$$

For  $L$  a multiple of 4, this is again a single-site perturbation for  $t = nv^{-1}$ ,  $n = 0, 1, 2, \dots$ , and interpolating smoothly in between. In this case, the non-differentiable curves in Figure 11 become smooth, but no other qualitative differences are observed.

Let us summarize the two regimes in terms of the two parameters  $v$  and  $B$ . We are in the adiabatic regime if  $Cv \ll 1$ . Since for small  $B$ , the adiabatic constant  $C$  is inverse proportional to  $B$ , we require  $v \ll B$ . For large  $B$  we know that  $C$  is proportional to  $B$  and thus we want that  $v \ll 1/B$ . The regime where the initial state is stationary is simply given by the condition that  $B \ll v$ .

## V. DMRG ALGORITHMS

### A. Ground state DMRG

The standard ground state DMRG algorithm [26] starts with the exact ground state on a small number of sites and obtains an approximation to the true ground

state on a large number  $L$  of sites by successively inserting new sites in the middle and truncating the number of states kept in the blocks to the left and right of the middle sites. The algorithm is well known and a comprehensive review exists [21], see also the book [20]. We highlight here the adaptations that are necessary because of the degeneracy and non-translation invariance of the ground states of the (translation invariant) XXZ kink Hamiltonian.

The degeneracy can be lifted by restricting to a sector of fixed total  $S^3$ -magnetization, but care has to be taken in growing the system. Consider for simplicity the analogous problem for Ising spins which can be up ( $+\frac{1}{2}$ ) or down ( $-\frac{1}{2}$ ) and take a four-site kink state with total magnetization 0 (see Figure 12, top). If we enlarge the system by inserting 2 sites in the middle we can again successfully target the zero magnetization kink (indicated by the dashed arrows) since the left and right blocks contain a good representation of the projection of the true zero magnetization kink on these blocks. On the other hand, if we want to target a kink with magnetization  $-1$ , we obviously cannot enlarge the  $-1$  kink on four sites in the usual way (see Figure 12, bottom) as the left and right blocks will not contain the correct states to approximate the true  $+1$  kink on six or more sites.

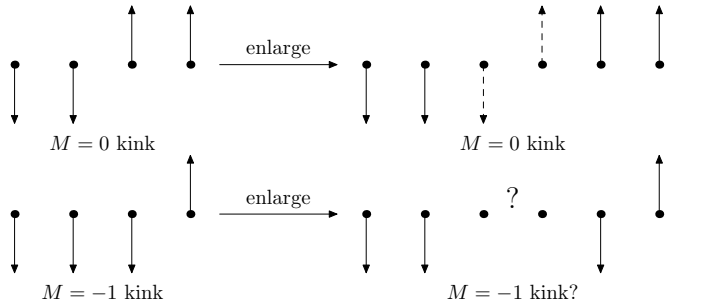


FIG. 12: Ising spin DMRG illustration, for magnetization=0 (left) and magnetization=-1 (right)

In general the solution is to always grow the system initially in the zero magnetization sector, with the interface located in between the two middle sites. If eventually a total magnetization with interface close to the middle is needed, this can be achieved by doing the finite system convergence sweeps in the new sector, with the zero magnetization state as initial trial state. If eventually an interface close to one of the edges is needed, this can be achieved by initially growing the system with zero magnetization, then at the right moment start growing the system at a magnetization which increases or decreases with one each step (effectively inserting two up or two down spins in the middle, thus shifting the kink to the right or left).

In the standard ground state DMRG algorithm, it is sufficient to compute the reduced density matrix on the left block only, and copy this to the right block by translation invariance. Here we compute separate reduced den-

sity matrices and block bases for both blocks. Targeting sectors of fixed magnetization is done by keeping truncated total  $S^3$ -magnetization operators for both left and right blocks, and computing the ground state of the truncated Hamiltonian in a specific sector of truncated total  $S^3$ .

The enlarging process implicitly assumes a translation invariant Hamiltonian. However, if the breaking of translation invariance is due to a local perturbation as in our case (with external magnetic fields located on one or two sites), we can grow the system targeting the zero magnetization kink, and add the perturbation for the finite system convergence sweeps where translation invariance is no longer needed. The DMRG state thus obtained converges indeed very rapidly to the true ground state of the perturbed Hamiltonian.

After the initial ground state computation, we have an approximation of the kink ground state with total  $S^3$ -magnetization zero on  $L$  sites, which can be expressed at will in any of the DMRG bases for left block length  $\ell = 0, 1, \dots, L-2$ . Due to the nature of our problem (the ground state has an interface exponentially localized around the middle and is very near to an all up/down state in the left/right block) we can get by with small block dimensions. Further justification for taking small block dimensions comes from [25], where it is argued that the success of DMRG is related to low entanglement entropy in one-dimensional systems. To recall this concept, let  $\rho$  be a state on the whole chain and  $\rho_L$  its restriction to a subinterval of  $m$  contiguous sites. Then the entanglement entropy is  $S(m) = -\text{tr} \rho_m \log(\rho_m)$ . Our Hamiltonians  $H(t)$  are non-critical with a positive mass gap. For zero magnetic field and  $\rho$  a kink state of definite magnetization,  $S(m) = 0$  due to the frustration free property. For non-zero magnetic field  $B$  this is not quite true but nevertheless we still have  $S(m) \rightarrow 0$  for large intervals around the support of  $B$ . This indicates why the block dimension  $\chi$  can be chosen rather small regardless of  $L$  and  $m$ .

## B. Time-dependent DMRG

To fix some notation, we give a more detailed overview of the algorithm for adaptive time-dependent DMRG (td-DMRG) [4, 6, 24, 27]. To obtain the initial state  $\psi(0)$  for the Schrödinger equation (5), which is the unique ground state of the Hamiltonian (4) at time  $t = 0$ , we perform a few sweeps through the system with the perturbed Hamiltonian (i.e., adding the perturbation field to the center sites nearest-neighbor Hamiltonian whenever the two center sites hit the middle of the chain), updating the DMRG block bases along the way.

The main idea of tdDMRG is that any operator  $A_{x,x+1}$  acting on two successive sites can be easily applied to a DMRG state by expressing it in the basis where the left block has length  $x-1$ , so the two untruncated center sites correspond to the two sites where  $A_{x,x+1}$  is acting

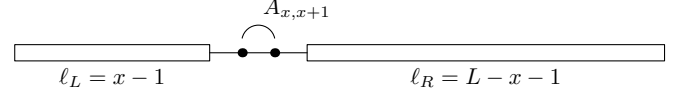


FIG. 13: DMRG block configuration for applying nearest-neighbor operator.

(see Figure 13). If  $H = \sum_x h_{x,x+1}$  is a nearest-neighbor Hamiltonian (not necessarily translation invariant) and  $\delta$  is a small number, the Heisenberg operator  $e^{-i\delta H}$  can be approximated by a second order Trotter decomposition

$$e^{-i\delta H} \approx e^{-\frac{1}{2}\delta h_{1,2}} e^{-\frac{1}{2}\delta h_{2,3}} \dots e^{-i\delta h_{L-1,L}} \dots e^{-\frac{1}{2}\delta h_{2,3}} e^{-\frac{1}{2}\delta h_{1,2}}. \quad (8)$$

So to apply  $e^{-i\delta H}$  to a DMRG state, we first write this state in the basis with the center sites all the way to the left and apply  $e^{-\frac{1}{2}\delta h_{1,2}}$ , then we rewrite the resulting state in the basis with the center sites shifted one site to the right and apply  $e^{-\frac{1}{2}\delta h_{2,3}}$ , etc. The name *adaptive* time-dependent DMRG comes from the fact that the DMRG basis is adapted to better represent the new state. This can be done after each application of a nearest-neighbor operator and shift to the right or left [6] or after each full time-step [23].

In the standard tdDMRG, adaptation of the basis is done by computing and truncating new reduced density matrices for the evolved state  $\psi(t)$ . In our problem the situation is different because we want to compute both the time evolved state  $\psi(t)$  and the true ground state  $\varphi(t)$  of  $H(t)$  and compare them (in the same DMRG basis, naturally), and we will use the ground state (or several low-lying states) of  $H(t)$  to adapt the Hilbert spaces.

The details of our algorithm are as follows. The time period  $[0, \tau]$  is first divided in  $n_\tau$  time steps of length  $\delta = \tau/n_\tau$  by discretizing the time evolution, i.e., the evolved states  $\psi(t)$  are defined by

$$\begin{aligned} \psi(0) &= \varphi(0), \\ \psi(n\delta) &= e^{-i\delta H(n\delta)} \psi((n-1)\delta), \quad n = 1, \dots, n_\tau. \end{aligned}$$

Each of these time steps is further divided into  $n_T$  smaller steps of length  $\delta_T = \delta/n_T$  for the Trotter decomposition, so

$$\psi(n\delta) \approx (e^{-i\delta_T H(n\delta)})^{n_T} \psi((n-1)\delta),$$

and  $e^{-i\delta_T H(n\delta)}$  is expanded as in (8). Note that only the interaction  $h_{L/2,L/2+1}$  is time-dependent. We shall call the so approximated state  $\psi_T(n\delta)$ .

Let us start at time 0 where  $\psi(0) = \varphi(0)$ . To apply  $e^{-i\delta H(\delta)}$  to it we need to have  $\psi(0)$  written in a DMRG basis that represents the low energy states of  $H(\delta)$ . To this end we use  $\varphi(0)$  as an initial trial state and apply standard finite system DMRG sweeps targeting the ground state  $\varphi(\delta)$  of  $H(\delta)$ , and update  $\psi(0)$  along the way. At the end of the sweeps we have a new DMRG basis for  $H(\delta)$ , its ground state  $\varphi(\delta)$ , and  $\psi(0)$  expressed in

the new basis. This is the *adaptive* part of our tdDMRG. Next we can apply  $e^{-i\delta H(\delta)}$  to the new representation of  $\psi(0)$  using the Trotter sweeping process and obtain the evolved state  $\psi_T(\delta)$ . By construction  $\psi_T(\delta)$  and  $\varphi(\delta)$  are expressed in the same DMRG basis, and their overlap and other quantities can be computed.

The subsequent time steps proceed in exactly the same manner. First the DMRG basis is adapted to the Hamiltonian  $H(n\delta)$  using the ground state  $\varphi((n-1)\delta)$  as an initial trial state;  $\psi_T((n-1)\delta)$  is updated along the way and thus expressed in the same basis as the new ground state  $\varphi(n\delta)$ ;  $e^{-i\delta H(n\delta)}$  is applied to  $\psi_T((n-1)\delta)$  by Trotter sweeps to obtain  $\psi_T(n\delta)$  which can then be compared to  $\varphi(n\delta)$ .

Although the motivation for adapting the DMRG bases in this way is inspired by the question to analyze the adiabatic approximation, we have found that it is also very convenient to compute the time-evolved state in the non-adiabatic regime. In this case, we need to keep more low-energy states, but we do not need to increase the block dimension, unlike standard tdDMRG which needs approximately twice the block dimension of ground state DMRG to achieve the same accuracy [27].

For the same entanglement entropy reason, the loss of norm due to truncation is very small even for long times and the main error comes from the Trotter approximation.

### C. Error analysis

Let  $\psi(t)$  be the true Schrödinger time evolution,  $\psi_T(t)$  be the second order Trotter approximation as above, and let  $\psi_{\text{ad}}(t)$  be the adiabatic time evolution of the state  $\psi$  at time  $t$ .  $\psi_{\text{ad}}(t)$  equals the ground state  $\varphi(t)$  up to a phase  $e^{i\alpha(t)}$ . For given velocity  $v$  we have  $\tau = 1/v$ .

To understand how well DMRG computes the adiabatic constant, we define two overlap functions,

$$o(v) = \min_{0 \leq t \leq 1/v} |\langle \psi(t), \psi_{\text{ad}}(t) \rangle|, \quad (9)$$

$$o_T(v) = \min_{0 \leq t \leq 1/v} |\langle \psi_T(t), \psi_{\text{ad}}(t) \rangle|. \quad (10)$$

This has the advantage that they are easily computed and do not depend on the phase. A simple calculation reveals that for normalized states  $\psi$  and  $\phi$ ,

$$\min_{\alpha \in [0, 2\pi]} \|\psi - e^{i\alpha} \phi\| = \sqrt{2(1 - |\langle \psi, \phi \rangle|)}.$$

Therefore the adiabatic constant,

$$\begin{aligned} C &= \lim_{v \rightarrow 0} v^{-1} \max_{0 \leq t \leq 1/v} \min_{\alpha(t) \in [0, 2\pi]} \|\psi(t) - e^{i\alpha(t)} \varphi(t)\| \\ &= \lim_{v \rightarrow 0} v^{-1} \sqrt{2(1 - o(v))}. \end{aligned}$$

In the case of our tdDMRG we have

$$C_T(v) = v^{-1} \sqrt{2(1 - o_T(v))}.$$

In order to calculate  $\psi_T(t)$  we have divided the whole time interval of length  $\tau$  into  $n_\tau$  subintervals of length one. That is just the discretization step. Before we apply the Trotter approximation we divide further into  $n_T$  subintervals of length  $1/n_T$ . On this interval, second order Trotter approximation gives an error of  $n_T^{-3} \max(1, B^2)$ . The total Trotter error is then of the order  $\xi = 1/(vn_T^2) \max(1, B^2)$ . More precisely, this means that with  $\psi_T = \psi_T(1/v)$ ,  $\psi = \psi(1/v)$ ,

$$\psi_T = (1 - \mathcal{O}(\xi^2))\psi + \mathcal{O}(\xi)\psi^\perp.$$

Therefore,

$$|\langle \psi_T, \psi_{\text{ad}} \rangle| = |\langle \psi, \psi_{\text{ad}} \rangle| + \mathcal{O}(\xi^2) + \mathcal{O}(\xi v).$$

since  $|\langle \psi^\perp, \psi_{\text{ad}} \rangle| \leq Cv$ . If we choose  $\xi \ll v$  then the above error is  $\mathcal{O}(\xi v)$ . Thus,

$$C_T = v^{-1} \sqrt{1 - |\langle \psi, \psi_{\text{ad}} \rangle|} (1 + \mathcal{O}(\frac{\xi}{v})).$$

This gives the condition  $|C_T - C| = \mathcal{O}(\frac{\xi}{v})$ . In our numerical computations we have used the parameter  $n_T = 100$  and  $v$  down to  $10^{-3}$  but we noticed very little difference (much less than 1%) to the adiabatic constant calculated with  $n_T = 10$ . Although the above estimate on  $|C - C_T|$  seems the best possible one, in practice the error is much smaller.

### D. Parameter values

As explained before, our problem is suitable for DMRG with small block dimension. We have verified that the algorithm converges up to machine precision to the true, known energies of the ground state and first excited state with block dimensions as low as 16 for a chain of length  $L = 20$ , and used this dimension for ground state as well as time-dependent computations. We carried out 3 system sweeps to obtain convergence of the ground states and of the DMRG bases at each time step. For given  $v$ , the final time  $\tau = 1/v$  was divided in time steps of length 1 which were further subdivided into 100 Trotter steps. For the ground state and adiabatic transport computations, we targeted the 3 lowest energy states of  $H(t)$  to construct the DMRG basis, increasing to the 5 lowest energy states for the fast changing magnetic field.

### E. Software

We have implemented the ground state and time-dependent DMRG algorithms in a Matlab® Toolbox which can be easily applied to other models than the Heisenberg model as well. The software is included in the tar archive with the tex source and the figure files which can be downloaded from [arxiv:cond-mat/0702059](http://arxiv:cond-mat/0702059).

## Acknowledgments

T.M. is a Postdoctoral Fellow of the Research Foundation – Flanders (Belgium). The research of B.N. is

supported in part by U.S. National Science Foundation grant # DMS-06-05342. W.S. is grateful for the support and hospitality at the International University Bremen, Germany.

---

[1] D.A Allwood, Gang Xiong, M.D. Cook, C.C. Faulkner, D. Atkinson, N. Vernier, and R.P. Cowburn, *Submicrometer ferromagnetic not gate and shift register*, *Science* **296** (2002), 2003–2006.

[2] G.S.D. Beach, C. Nistor, C. Knutson, M. Tsoi, and J.L. Erskine, *Dynamics of field-driven domain-wall propagation in ferromagnetic nanowires*, *Nature* **4** (2005), 741–744.

[3] P. Contucci, B. Nachtergael, and W.L. Spitzer, *The ferromagnetic Heisenberg XXZ chain in a pinning field*, *Phys. Rev. B* **66** (2002), 0644291–13.

[4] A. J. Daley, C. Kollath, U. Schollwoeck, and G. Vidal, *Time-dependent density-matrix renormalization-group using adaptive effective Hilbert spaces*, *J. Stat. Mech.: Theor. Exp.* (2004), P04005.

[5] M. Fannes, B. Nachtergael, and R. F. Werner, *Finitely correlated states of quantum spin chains*, *Commun. Math. Phys.* **144** (1992), 443–490.

[6] D. Gobert, C. Kollath, U. Schollwöck, and G. Schütz, *Real-time dynamics in spin-(1/2) chains with adaptive time-dependent density matrix renormalization group*, *Phys. Rev. E* **71** (2005), 036102.

[7] C.-T. Gottstein and R. F. Werner, *Ground states of the infinite  $q$ -deformed Heisenberg ferromagnet*, Preprint.

[8] C.F. Hirjibehedin, C.P. Lutz, and A.J. Heinrich, *Spin coupling in engineered atomic structures*, *Science* **312** (2006), 1021–1024.

[9] S. Jansen, M.B. Ruskai, and R. Seiler, *Bounds for the adiabatic approximation with applications to quantum computation*, preprint.

[10] T. Kato, *On the adiabatic theorem of quantum mechanics*, *Journ. Phys. Soc. Jap.* **5** (1955), 435–439.

[11] A.Yu. Kitaev, A.H. Shen, and M.N. Vyalyi, *Classical and quantum computation*, Graduate Studies in Mathematics, vol. 47, American Mathematical Society, 2002.

[12] T. Koma and B. Nachtergael, *The spectral gap of the ferromagnetic XXZ chain*, *Lett. Math. Phys.* **40** (1997), 1–16.

[13] ———, *The complete set of ground states of the ferromagnetic XXZ chains*, *Adv. Theor. Math. Phys.* **2** (1998), 533–558.

[14] A. Messiah, *Quantum mechanics*, Dover Publications, 1999.

[15] B. Nachtergael, W. Spitzer, and S. Starr, *Ferromagnetic ordering of energy levels*, *Journ. Stat. Phys.* **116** (2004), 719–738.

[16] ———, *Droplet Excitations for the Spin-1/2 XXZ Chain with Kink boundary Conditions*, To appear in *Ann. Henri Poincaré*; DOI 10.1007/s00023-006-0304-6, 2006.

[17] B. Nachtergael and S. Starr, *Droplet states in the XXZ Heisenberg model*, *Commun. Math. Phys.* **218** (2001), 569–607.

[18] T. Ono, H. Miyajima, K. Shigeto, K. Mibu, N. Hosono, and T. Shinjo, *Propagation of a magnetic domain wall in a submicrometer magnetic wire*, *Science* **284** (1999), 468–470.

[19] V. Pasquier and H. Saleur, *Common structures between finite systems and conformal field theories through quantum groups*, *Nuclear Physics B* **330** (1990), 523–556.

[20] I. Peschel, X. Wang, M. Kaulke, and K. Hallberg (eds.), *Density-matrix renormalization - a new numerical method in physics*, Lecture Notes in Physics, vol. 528, Springer, 1999.

[21] U. Schollwöck, *The density-matrix renormalization group*, *Rev. Mod. Phys.* **77** (2005), 259.

[22] W. Thirring, *Quantum mathematical physics: Atoms, molecules and large systems*, Springer, 2003.

[23] F. Verstraete, J. J. Garca-Ripoll, and J. I. Cirac, *Matrix product density operators: Simulation of finite-temperature and dissipative systems*, *Phys. Rev. Lett.* **93** (2004), 207204.

[24] G. Vidal, *Efficient simulation of one-dimensional quantum many-body systems*, *Phys. Rev. Lett.* **93** (2004), no. 4, 040502.

[25] G. Vidal, J.I. Latorre, E. Rico, and A. Kitaev, *Entanglement in quantum critical phenomena*, *Phys. Rev. Lett.* **90** (2003), no. 22, 227902.

[26] S. R. White, *Density-matrix algorithms for quantum renormalization groups*, *Phys. Rev. B* **48** (1993), no. 14, 10345–10356.

[27] S. R. White and A. E. Feiguin, *Real time evolution using the density matrix renormalization group*, *Phys. Rev. Lett.* **93** (2004), 076401.